



Genetic Regulation of Root Hair Development in *Arabidopsis Thaliana*: A Network Model

LUIS MENDOZA AND ELENA R. ALVAREZ-BUYLLA*

*Laboratorio de Genética Molecular y Evolución, Instituto de Ecología UNAM, Ap. Postal 70-275,
Coyoacán, D.F. CP04510, Mexico*

(Received on 24 June 1999, Accepted in revised form on 31 January 2000)

The root epidermis of *Arabidopsis thaliana* is formed by alternate files of hair and non-hair cells. Epidermal cells overlying two cortex cells eventually develop a hair, while those overlying only one cortex cell do not. Here we propose a network model that integrates most of the available genetic and molecular data on the regulatory and signaling pathways underlying root epidermal differentiation. The network architecture includes two pathways; one formed by the genes *TTG*, *R* homolog, *GL2* and *CPC*, and the other one by the signal transduction proteins *ETR1* and *CTR1*. Both parallel pathways regulate the activity of *AXR2* and *RHD6*, which in turn control the development of root hairs. The regulatory network was simulated as a dynamical system of eight discrete state variables. The distinction between epidermal cells contacting one or two cortical cells was accounted for by fixing the initial states of *CPC* and *ETR1* proteins. The model allows for predictions of mutants and pharmacological effects because it includes the ethylene receptor. The dynamical system reaches one of the six stable states depending upon the initial state of the *CPC* variable and the ethylene receptor. Two of the stable states describe the activation patterns observed in mature trichoblasts (hair cells) and atrichoblasts (non-hair cells) in the wild-type phenotype and under normal ethylene availability. The other four states correspond to changes in the number of hair cells due to experimentally induced changes in ethylene availability. This model provides a hypothesis on the interactions among genes that encode transcription factors that regulate root hair development and the proteins involved in the ethylene transduction pathway. This is the first effort to use a dynamical system to understand the complex genetic regulatory interactions that rule *Arabidopsis* primary root development. The advantages of this type of models over static schematic representations are discussed.

© 2000 Academic Press

Introduction

The increasing amount of data on the molecular mechanisms underlying cellular differentiation and morphogenesis are putting forward complex networks of genetic interactions. These are dynamical systems that operate in specific cellular

and spatial scales. Network models of genetic regulatory interactions are dynamical representations of molecular interactions, and can be used to predict the stable activation states attained by a given genetic architecture within mature cells (Kauffman, 1993). These models provide a formal dynamical framework to analyse cellular differentiation, in contrast to schematic representations of gene and protein

* Author to whom correspondence should be addressed.
E-mail: abuylla@servidor.unam.mx

interactions often published in experimental papers. However, network models for specific biological systems are still scarce (for notable examples see Bodnar, 1997; Reinitz & Sharp, 1995). In this paper, we propose a network model for cell differentiation during root epidermis development of the experimental plant system *Arabidopsis thaliana*.

In contrast to most animals, plant cells cannot move, while positional cues are important in ruling cellular fate. Also, plant organ development is remarkably plastic in response to environmental conditions (Meyerowitz, 1997; Pigliucci, 1996; Scheres & Wolkenfelt, 1998). Therefore, cell signaling should play important roles in plant cellular specification and pattern formation, which take place in shoot and root meristems, where organs continuously develop (Scheres, 1997). Within floral meristems, transcription factors are known to be involved in regional specification (Coen & Meyerowitz, 1991; Weigel & Meyerowitz, 1993), but the gene products required for the signaling processes during pattern formation are only starting to be studied. The complexity of the shoot meristem, however, hinders the experimental approaches that are required to understand the role of cell signaling during development. In contrast, the regular cellular architecture, small size and transparency of the *Arabidopsis* root meristem, enables the combination of genetic, cell ablation and micro-injection approaches to study the signaling mechanisms involved in cell specification (see Scheres, 1996, 1997). This makes the root a particularly attractive system to develop mechanistic models, which help understand how molecular signals and cellular interactions are integrated across cells during development.

The root epidermis of *Arabidopsis* is an exceptionally simple system to address questions regarding the cellular and genetic mechanisms that determine a stereotyped pattern of cellular differentiation. The root epidermis is made of alternate columns of hair cells (trichoblasts) and non-hair cells (atrachoblasts). Cell fate is determined by the relative location of epidermal cells with respect to the cortex cell walls. Recent studies in the root of *Arabidopsis* have identified at least four transcription factors that regulate root hair development, and the ethylene signaling

pathway as one of the signaling mechanisms involved in it (see Scheres & Wolkenfelt, 1998). It is unclear if ethylene is a molecule available to all epidermal cells, or if it forms a gradient conveying positional information during sub-specification of epidermal cell types. Additional experimental results are necessary to solve the details of the interplay between transcriptional regulation and ethylene transduction pathway; however, to integrate all the data available to date we put forward the first genetic regulatory network model for root hair development.

No previous model has proposed a genetic regulatory mechanism responsible for the cellular patterning observed in the *Arabidopsis* root epidermis. In this paper, we propose a regulatory network model of discrete states that may be used as a framework to predict the effect of mutations that alter root hair formation. The network is implemented as a dynamical system with discrete state variables. Departing from any initial activation state, the model reaches one of six stable activation patterns. Two of these correspond to stable activation states that characterize mature hair and non-hair cells under wild type conditions. The other four correspond to genetic patterns that would diminish or augment the trichoblasts to atrichoblasts ratio according to induced changes in ethylene availability. This model contrasts in two important ways with our previous models of flower development (Mendoza & Alvarez-Buylla, 1998; Mendoza *et al.*, 1999). First, in our previous network implementations we used the ABC model of flower morphogenesis to translate the steady gene activation patterns into flower morphology (Coen & Meyerowitz, 1991; Meyerowitz, 1994). In this study, we lack a morphogenetic model for root hair formation, and we used the activation state of the most downstream elements of the regulatory network (RHD6 and AXR2) to establish cell fate (i.e trichoblasts or atrichoblasts). Second, the flower models were treated as autonomous dynamical systems in which no links with extra-cellular signals were postulated. In this case, however, we postulate a link with external signals via the response of the elements representing CPC and ETR1. Such responses are incorporated by fixing the initial states of these

two elements in the network, in such a way that the appearance of root hairs is determined by the position of epidermal cells relative to that of cortical cells. This is the first dynamical model that is able to describe the effect of mutations as well as pharmacological treatments on the cellular patterning in the root epidermis.

The Root of *Arabidopsis*

The mature root of *Arabidopsis* consists of single concentric layers of cells, which from the periphery to the centre form the epidermis, cortex, endodermis and pericycle, surrounding vascular tissues (Fig. 1). Root meristem tissues are organized in longitudinal cell files. Mature cells are located distal to the root tip, while immature cells are near the root tip. Along this gradient, that goes from the root tip to the plant base, four regions have been defined: the division, the slow elongation, the fast elongation, and the differentiation zones (Berger *et al.*, 1998b). Each cell file is maintained by elongation and subsequent anticlinal division (with the division plane perpendicular to the growth axis) of initial cells. There are four types of initial cells: epidermis/lateral-root cap, cortex/endodermis, provascular and columella initials, whose daughter cells are able to divide and differentiate into one of the mature cell types forming the different root tissues (Dolan *et al.*, 1993, 1994). Epidermal cells

undergo a further process of differentiation. Cells that contact the anticlinal cell wall between two cortical cells differentiate into root hair cells. In contrast, developing epidermal cells contacting the periclinal wall of a single cortical cell differentiate into mature hairless cells. The hair is a tubular extension that develops in trichoblasts, but its presence is not the only morphological difference with atrichoblasts. From a very early stage of development, trichoblasts have a more densely staining cytoplasm, a reduced vacuolation and are shorter than atrichoblasts (Berger *et al.*, 1998b; Dolan *et al.*, 1994).

Molecular and Genetic Basis of the Regulatory Network Model

We present a network model that integrates most of the published genes involved in root epidermis development for which regulatory interactions could be inferred. We first review the experimental evidence that supports the proposed regulatory network architecture. The model includes genes that encode transcription factors and regulatory proteins. In some cases, transcriptional and post-transcriptional regulation could not be distinguished based on available data. Therefore, if an element of the network model is "off", it represents either a null transcriptional gene activity or an inactive protein. Despite being biologically relevant, the ambiguity on the molecular mechanism does not affect the dynamical result, because the particular nature of functionality (or lack of it) is irrelevant for the study of the collective behavior of interdependent elements. For a review on the known molecular nature of many mutations see Van den Berg *et al.* (1998). Throughout the text, genes coding for known proteins are in upper-case italics (*TTG*, *R* homolog, *GL2* and *CPC*) and known and unknown proteins are in upper-case normal text (*ETR1*, *CTR1*, *RHD6*, and *AXR2*). Wild type and mutated genes are indicated with upper- and lower-case letters, respectively.

TRANSPARENT TESTA GLABRA (TTG) is a gene coding for a WD40 protein involved in root hair development, and its loss-of-function mutation results in plants with hairs throughout the epidermis (Galway *et al.*, 1994; Walker *et al.*,

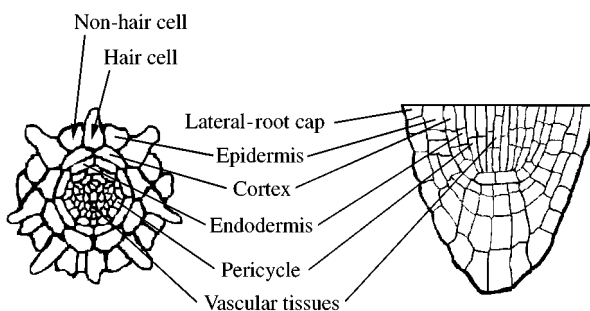


FIG. 1. Schematic representation of transverse (left) and longitudinal (right) midsections of the *Arabidopsis thaliana* root. The primary root is formed by concentric layers of lateral root cap, epidermis, cortex, endodermis, and pericycle surrounding vascular tissues. The transverse section represents a region where the lateral-root cap has detached and root hairs begin to grow. Epidermal cells contacting one and two cortical cells differentiate into Non-hair and Hair, respectively. Mature trichoblasts develop a root hair.

cited in Hung *et al.*, 1998). *TTG* is an important activator of *GLABRA2* (*GL2*), mRNA is expressed inside atrichoblasts in wild type plants. Like *ttg* plants, *gl2* mutants have hairs throughout the epidermis. However, *gl2* epidermal cells can be distinguished as trichoblasts or atrichoblasts based on vacuolation and cytoplasmic density, while *ttg* epidermal cells cannot (Galway *et al.*, 1994; Masucci *et al.*, 1996; Masucci & Schiefelbein, 1996; Schiefelbein *et al.*, 1997). *GL2* encodes a homeodomain protein that probably functions as a transcription factor of genes involved in determining the hairless cellular fate. *TTG* is one of the important activators of *GL2*, because its expression is markedly reduced in *ttg* mutants (Di Cristina, 1996; Hung *et al.*, 1998). However, the activation of *GL2* by *TTG* seems to be mediated by another gene product. In *Arabidopsis*, over-expression of the corn *R* cDNA (a *myc* gene), under the control of the cauliflower mosaic virus 35S promoter, suppresses the *ttg* phenotype (Galway *et al.*, 1994). Such information suggests that an *Arabidopsis R* homolog is acting downstream of *TTG*. Moreover, transgenic 35S::*R GL2*::*GUS* plants show *GUS* activity throughout the epidermis, lateral root cap cells and cortical cells, while 35S::*R gl2* plants show a *gl2* phenotype (Hung *et al.*, 1998). All this evidence supports that *TTG* activates an *Arabidopsis R* homolog, which in turn activates *GL2* [Fig. 2(a)].

TTG is not the only regulator of *GL2*; *GL2*::*GUS ttg* seedlings exhibit a significant reduction, but not a total loss, of *GUS* activity. Interestingly, the remaining *GL2*::*GUS* activity is found in the atrichoblasts, where *GL2* is normally expressed (Hung *et al.*, 1998). Therefore, the *ttg* mutation affects the level of *GL2* expression but not its spatial localization. These results suggest that an additional *TTG*-independent pathway restricts the *GL2* expression to atrichoblasts. Such an alternative pathway might be mediated by *CAPRICE* (*CPC*) that is a putative transcription factor preferably expressed in atrichoblasts, although it is also present in trichoblasts at lower levels, as revealed by *GUS* staining and *in situ* hybridizations (Wada *et al.*, 1997, 1998). The *cpc* mutants express *GL2* in almost all epidermal cells and have few irregularly distributed root hairs, while 35S::*CPC* plants have root hairs in all

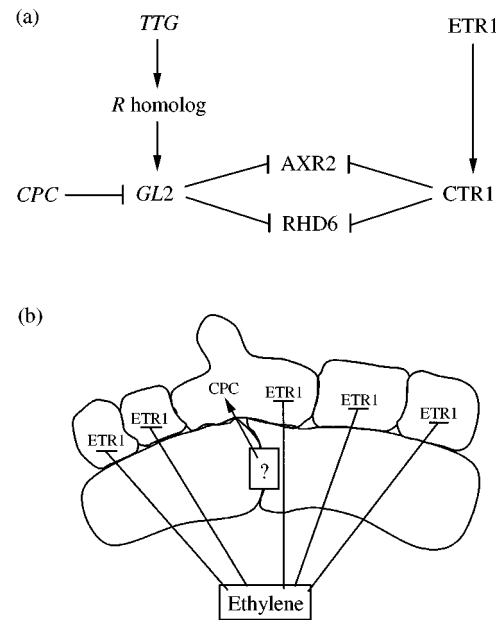


FIG. 2. (a) Architecture of the genetic regulatory network model for hair development in the *Arabidopsis* root epidermis. Arrows and blunt-lines represent activation and repression, respectively. (b) Assumption of signals affecting the activity of the regulatory network. Ethylene availability, acting upon its receptor *ETR1*, is assumed to be uniform across epidermal cells under normal conditions and pharmacological treatments (—). An unknown protein expressed along the longitudinal anticlinal cell walls of the cortex cells (? →) is assumed to make the *CPC* protein active or available in cells overlying two cortical cells.

epidermal cells like the *gl2* or *ttg* mutant phenotypes. Also, *cpc gl2* double mutants have the same phenotype as *gl2* single mutants (Wada *et al.*, 1997). Put together, this evidence indicates that *CPC* is a negative regulator of *GL2* [Fig. 2(a)]. *CPC* and *TTG* regulate *GL2* via two different pathways, because *cpc ttg* roots have an intermediate phenotype compared to each of the single mutants (Wada *et al.*, 1997).

It is strange that while *CPC* mRNA is expressed mainly in atrichoblasts its null mutants have altered development of trichoblasts. There are several possible molecular mechanisms to explain these apparently contradictory results. One possibility is that *CPC* is a non-autonomous inhibitor of the non-hair fate, in which case the model would imply a lateral signaling inhibition mechanism. Such a model is somewhat challenged by cell ablation experiments, that suggest that the root-hair cell fate does not depend on

signaling from neighboring epidermal cells (non-hair cells) (Berger *et al.*, 1998a). Instead, this and additional available data (Berger *et al.*, 1998b), suggest that a signaling mechanism emerging from the anticlinal cell walls in the cortex is critical for cell patterning in the epidermis. Such a signaling mechanism seems to affect the availability or activity of the protein encoded by *CPC*, rather than the presence of its mRNA. The fact that *35S::CPC* plants have ectopic hairs in cells that do not contact anticlinal cortical cell walls, might be explained if such an over-expression saturates or bypasses the pathway that regulates the activity or availability of CPC protein. Hence in Fig. 2, *CPC* in hair-cells refers to the availability of active CPC protein, rather than to its mRNA expression, that has been reported to be higher in atrichoblasts (Wada *et al.*, 1998). However, additional data are needed to clearly discern this and a lateral inhibition model to explain the difference between the observed CPC mRNA and the CPC protein activity.

Members of the ethylene receptor family share sequence similarity, and mutations in any of them have a similar ethylene-insensitive phenotype (Hua *et al.*, 1995; Hua & Meyerowitz, 1998). Analyses of single and multiple mutants showed that *ETHYLENE RESISTANT 1 (ETR1)*, *ETHYLENE RESISTANT 2 (ETR2)*, *ETHYLENE INSENSITIVE 4 (EIN4)* and *ETHYLENE RESPONSE SENSOR 2 (ERS2)* have redundant functions in the ethylene signaling pathway (Hua & Meyerowitz, 1998). The most studied member of such a family is *ETR1*, which is a membrane protein very similar to the bacterial two-component histidine kinases (for recent reviews see Fluhr, 1998; Kieber, 1997). We have included only the *ETR1* protein in our model because the ethylene-binding activity has been demonstrated solely for this receptor. However, it should be kept in mind that the *in vivo* response to ethylene is probably mediated by the formation of multiple complexes (reviewed in Johnson & Ecker, 1998). It is known that *ETR1* acts upstream of *CONSTITUTIVE TRIPLE RESPONSE 1 (CTR1)*, Kieber, 1997), and *ETR1* seems to be an activator of *CTR1* [Fig. 2(a)] because loss-of-function mutants of the ethylene receptor family and *ctr1* mutants are similar (Hua & Meyerowitz, 1998). Finally, in contrast with the typical mechanism of hormone

action, ethylene *represses* the activity of the receptor complex upon binding, which in turn activates *CTR1* (Hua & Meyerowitz, 1998). Although the net effect of ethylene is the inhibition of *CTR1*, its specific mechanism of action is relevant for the specification of the model (see ahead).

The ethylene response pathway plays a major role in root hair appearance and development (Tanimoto *et al.*, 1995). Such a pathway has been partially uncovered, and includes the gene *CTR1*. Plants with the *ctr1* mutation have ectopic root hairs; however in contrast to *ttg* and *gl2* plants, they have only a slight increase in the proportion of hair to non-hair cells (Dolan *et al.*, 1994). The *CTR1* gene encodes a putative serine-threonine kinase, and the phenotype of *ctr1* mutants suggests that the *CTR1* protein negatively regulates the ethylene signaling pathway (Kieber *et al.*, 1993; Scheres, 1997). Also, it is known that *CTR1* acts downstream of the ethylene receptor family. The family of genes encoding different forms of the ethylene receptor includes *ETR1*, *ETR2*, *EIN4*, *ERS1* and *ERS2*. *In vitro* assays have shown that *CTR1* interacts with, at least, *ETR1* and *ERS1* proteins (Clark *et al.*, 1998).

AUXIN RESISTANT2 (AXR2) and *ROOT HAIR DEFECTIVE6 (RHD6)* are also involved in root hair development but they seem to be part of two different pathways downstream of *GL2*. Both single *axr2* and *rhd6* mutants have fewer root hairs than wild-type plants, while double *axr2 rhd6* mutants completely lack root hairs, suggesting that *AXR2* and *RHD6* form part of two separate pathways. However, the pathway including *RHD6* seems to be more important than that of *AXR2*, because *rhd6* mutants have fewer hairs than *axr2* mutants (see ahead). Double *axr2 ttg* and *axr2 gl2* mutants have the same phenotype as *axr2* plants (Masucci & Schiefelbein, 1996), suggesting that *AXR2* is downstream of the *TTG/GL2* pathway. We propose that *GL2* inhibits the *AXR2* gene, or alternatively, inactivates the *AXR2* product [Fig. 2(a)]. This ambiguity is not problematic for defining the model because the mathematical treatment is identical in both cases.

In contrast, *ttg rhd6* and *gl2 rhd6* mutants have more hairs than *rhd6*, but clearly fewer than *ttg*

or *gl2* plants (Masucci & Schiefelbein, 1996). This partial suppression of the *ttg* and *gl2* phenotypes could indicate that *RHD6* is regulated by a pathway independent of that of *GL2*. However, the data from transgenics bearing *35S::R* homolog constructs suggest that *RHD6* is downstream of *TTG* and *GL2*. Seedling roots containing *35S::R* and *GL2::GUS* constructs have ectopic GUS activity compared to wild-type pattern, demonstrating that constitutive expression of the myc-like *R* gene by the *35S* promoter is sufficient to induce ectopic *GL2*-promoter activity during root development (Huang *et al.*, 1998). We use this evidence to infer the possible interaction between *RHD6* and *GL2*. An over-expression of *GL2* in these *35S::R* lines, would produce a reduction of *AXR2* and *RHD6* expression if both were negatively regulated by *GL2*. If this is the case, *35S::R* plants would have a similar (not identical because the ethylene signal transduction pathway also regulates *RHD6* and *AXR2*) phenotype to that of *axr2 rhd6* double-mutant plants. Indeed, *35S::R* transformants have roots almost deprived of root hairs and their trichoblast files have an altered early fate specification (Berger *et al.*, 1998b) as do the double *axr2 rhd6* mutants.

The data by Galway *et al.* (1994) also support that *RHD6* is downstream of *GL2*. Landsberg wild-type plants have 61.5 ± 7.7 root hairs mm^{-1} and *ttg 35S::R* transgenic plants, which are identical to *35S::R* transgenics, have only 2.3 ± 3.1 root hairs mm^{-1} . The latter phenotype is much more similar to the double *rhd6 axr2* mutants, which hardly has any root hairs, than to the single *axr2* mutant, that has 27 ± 4 hairs mm^{-1} . The latter phenotype would be expected if *RHD6* was not downstream of *GL2*. Therefore, we conclude that *RHD6* is negatively regulated by *GL2*. Furthermore, *gl2 rhd6* mutants have more hairs than *rhd6*, suggesting that there is an *RHD6*-independent pathway altering root hair appearance. These phenotypes further support that *RHD6* is inhibited by *GL2* but in a separate pathway from that of *AXR2* [Fig. 2(a)]. However, the inhibition of *RHD6* by *GL2* seems to be weaker than that of *AXR2*, because the difference in the number of root hairs between *axr2* and *axr2 gl2* mutants is larger than the difference between *rhd6* and *rhd6 gl2* mutants. Finally, the fact that *GL2::GUS* expression is not altered by

mutations in *AXR2*, *RHD6*, or even *GL2* (Masucci & Schiefelbein, 1996) suggests that there is no feedback from *RHD6* or *AXR2* to *GL2*.

RHD6 and *AXR2* seem to connect the transcriptional regulation pathway determining cell fate in the root epidermis (i.e. trichoblasts or atrichoblasts) to the ethylene response pathway via *GL2*. ACC, the direct precursor of ethylene, induces the appearance of root hairs in a dose-dependent manner in wild-type plants (Tanimoto *et al.*, 1995). The hairless *rhd6* and *axr2* single mutants almost recover the wild-type phenotype when treated with ACC. However, ACC addition does not induce root hair formation in *rhd6 axr2* double mutants (Masucci & Schiefelbein, 1996). These data suggest that *RHD6* and *AXR2* are downstream of the ethylene response pathway. Such a pathway from the ethylene receptor to *RHD6* and *AXR2* should be independent of *GL2*, because ACC treatment does not alter *GL2* expression (Masucci & Schiefelbein, 1996). We propose that CTR1 represses *AXR2* and *RHD6* independently of *GL2* [Fig. 2(a)]. We do not know, however, if such a negative regulation is exerted at a transcriptional level or directly on the protein.

The files of epidermal cells are created by anticlinal divisions and a constant number of epidermal files is maintained. However, sometimes an epidermal cell (often a trichoblast) divides longitudinally originating an extra file. Trichoblasts do not express *GL2* before an abnormal division. However, in the resulting daughter cell that overlies only one cortical cell, *GL2* becomes active (Fig. 5 in Berger *et al.*, 1998b). *GL2* and *CPC* are both expressed at the mRNA level in atrichoblasts (Wada *et al.*, 1997), but *CPC* protein seems to be active in trichoblasts only, although here its mRNA levels are low. In the new atrichoblasts, the *CPC* protein could be either sequestered in the cytoplasm or it could be in an inactive form. Developing trichoblasts and atrichoblasts, spatially isolated from other trichoblasts, other atrichoblasts or cortical cells, continue with their normal division and development into mature hair or non-hair epidermal cells respectively, as evidenced by molecular and morphological markers (Berger *et al.*, 1998a). But the development of a hair cell should involve an external signal that makes the *CPC* protein available or active and inhibits *GL2*.

The network model incorporates the effect of extra-cellular signals that modify the activation state of two network elements: the CPC and ETR1 proteins. The initial states of these determine which attractor is reached. Each attractor is a particular pattern of stable gene activation, including *AXR2* and *RHD6*. Moreover, the activation state of *AXR2* and *RHD6* can be translated into a particular phenotype. We determined the initial state of CPC based on the location of cells. Epidermal cells that contact two cortical cells have active or available protein encoded by *CPC* (initial state = 1) while those that contact only one cell do not have active or available protein encoded by this gene (initial state = 0). Also, we assumed that the ethylene supply, and therefore the ethylene receptor activity, are maintained constant and uniform throughout the epidermis [Fig. 2(b) and see discussion ahead]. In our model, we set ETR1 = 1 to simulate the wild-type activation level of ethylene receptor in both trichoblasts and atrichoblasts. On the contrary, to simulate pharmacological treatments we have set ETR1 initial states to 0 and 2, to model the addition of ethylene (or ACC) and AVG, respectively. This is because ethylene inhibits the activity of its own receptor, while AVG inhibits ethylene synthesis and thus leads to an over-activation of the ethylene receptor. Based on experimental evidence at hand, we assumed that the ethylene supply and the ethylene receptor activity are maintained constant and uniform throughout the epidermis [Fig. 2(b), and see discussion ahead].

Finally, according to the available molecular evidence in both normal and abnormal division patterns, *TTG* should be constitutively expressed in the root epidermis, while the active protein encoded by *CPC* should be present only in cells overlying two cortical cells [see Fig. 2(b)]. Our model incorporates both hypotheses. The constitutive expression of *TTG* could be maintained by a positive self-regulation after its induction during embryonic development. One possible way to attain the localized activity or availability of the protein encoded by *CPC* is by means of a diffusible signal such as ethylene, capable of crossing between the junction of longitudinal anticlinal cell walls, but not through them (Tanimoto *et al.*, 1995). However, a more

plausible mechanism could involve a molecule specifically expressed in the anticlinal cell walls, capable of inducing the activation or the liberation of the protein encoded by *CPC* in the contacting epidermal cells.

Simulations

Figure 3 shows the transition tables for each one of the elements included in the regulatory network. Half of the network elements are binary variables, while network elements involved in the ethylene-response pathway are modeled as three-state variables. The three-state elements enable the simulation of the differential response of roots to ACC (the direct precursor of ethylene) or AVG (an inhibitor of ethylene synthesis) treatments. All the tables in Fig. 3 could be united into a single transition table for the entire network, thus defining the entire dynamical behavior of the system. However, this is not practical because a complete table would have 1296 rows. Nevertheless, we present in Table 1 the final activation

<p>(a)</p> <table border="1" style="margin-left: auto; margin-right: auto;"> <thead> <tr> <th>t</th> <th>$t+1$</th> </tr> </thead> <tbody> <tr> <td>TTG</td> <td>Rh</td> </tr> <tr> <td>0</td> <td>0</td> </tr> <tr> <td>1</td> <td>1</td> </tr> </tbody> </table>	t	$t+1$	TTG	Rh	0	0	1	1	<p>(b)</p> <table border="1" style="margin-left: auto; margin-right: auto;"> <thead> <tr> <th>t</th> <th>t</th> <th>$t+1$</th> </tr> </thead> <tbody> <tr> <td>Rh</td> <td>CPC</td> <td>GL2</td> </tr> <tr> <td>0</td> <td>0</td> <td>0</td> </tr> <tr> <td>0</td> <td>1</td> <td>0</td> </tr> <tr> <td>1</td> <td>0</td> <td>1</td> </tr> <tr> <td>1</td> <td>1</td> <td>0</td> </tr> </tbody> </table>	t	t	$t+1$	Rh	CPC	GL2	0	0	0	0	1	0	1	0	1	1	1	0																
t	$t+1$																																										
TTG	Rh																																										
0	0																																										
1	1																																										
t	t	$t+1$																																									
Rh	CPC	GL2																																									
0	0	0																																									
0	1	0																																									
1	0	1																																									
1	1	0																																									
<p>(c)</p> <table border="1" style="margin-left: auto; margin-right: auto;"> <thead> <tr> <th>t</th> <th>$t+1$</th> </tr> </thead> <tbody> <tr> <td>ETR1</td> <td>CTR1</td> </tr> <tr> <td>0</td> <td>0</td> </tr> <tr> <td>1</td> <td>1</td> </tr> <tr> <td>2</td> <td>2</td> </tr> </tbody> </table>	t	$t+1$	ETR1	CTR1	0	0	1	1	2	2	<p>(d)</p> <table border="1" style="margin-left: auto; margin-right: auto;"> <thead> <tr> <th>t</th> <th>t</th> <th>$t+1$</th> <th>$t+1$</th> </tr> </thead> <tbody> <tr> <td>GL2</td> <td>CTR1</td> <td>RHD6</td> <td>AXR2</td> </tr> <tr> <td>0</td> <td>0</td> <td>2</td> <td>2</td> </tr> <tr> <td>0</td> <td>1</td> <td>2</td> <td>1</td> </tr> <tr> <td>0</td> <td>2</td> <td>1</td> <td>0</td> </tr> <tr> <td>1</td> <td>0</td> <td>1</td> <td>1</td> </tr> <tr> <td>1</td> <td>1</td> <td>0</td> <td>0</td> </tr> <tr> <td>1</td> <td>2</td> <td>0</td> <td>0</td> </tr> </tbody> </table>	t	t	$t+1$	$t+1$	GL2	CTR1	RHD6	AXR2	0	0	2	2	0	1	2	1	0	2	1	0	1	0	1	1	1	1	0	0	1	2	0	0
t	$t+1$																																										
ETR1	CTR1																																										
0	0																																										
1	1																																										
2	2																																										
t	t	$t+1$	$t+1$																																								
GL2	CTR1	RHD6	AXR2																																								
0	0	2	2																																								
0	1	2	1																																								
0	2	1	0																																								
1	0	1	1																																								
1	1	0	0																																								
1	2	0	0																																								

FIG. 3. Transition tables for the network variables: (a) Rh (the *Arabidopsis* homolog of the corn R element), (b) *GL2*, (c) *CTR1*, and (d) *RHD6* and *AXR2*. Variable *TTG* is assumed to be constitutively active (see main text), or always inactive if mutated. The state of variable ETR1 reflects the level of available ethylene; under wild-type conditions ETR1 is set to 1. To simulate treatments with increased ethylene or ACC, ETR1 is set to zero. Conversely, a decrease of ethylene availability, or the addition of AVG, is achieved by setting ETR1 to 2. Finally, *CPC* is set to 1 for cells in direct contact with two cortical cells, and set to 0 in those contacting only one cortical cell.

TABLE 1
Basins of attraction and attractors of the network model

Genotype	Basins of attraction (initial states)	Attractors (final steady states)
Wild type	XX0X1XXX	11011100*
	XX1X1XXX	11101121**
	XX0X0XXX	11010011†
	XX1X0XXX	11100022††
	XX0X2XXX	11012200‡
	XX1X2XXX	11102210‡‡
<i>ttg</i>	XX0X1XXX	00001121*
	XX1X1XXX	00101121**
	XX0X0XXX	00000022†
	XX1X0XXX	00100022††
	XX0X2XXX	00002210‡
	XX1X2XXX	00102210‡‡
<i>R homolog</i>	XX0X1XXX	10001121*
	XX1X1XXX	10101121**
	XX0X0XXX	10000022†
	XX1X0XXX	10100022††
	XX0X2XXX	10002210‡
	XX1X2XXX	10102210‡‡
<i>cpc</i>	XXXX1XXX	11011100*
	XXXX0XXX	11010011†
	XXXX2XXX	11012200‡
<i>gl2</i>	XX0X1XXX	11001121*
	XX1X1XXX	11101121**
	XX0X0XXX	11000022†
	XX1X0XXX	11100022††
	XX0X2XXX	11002210‡
	XX1X2XXX	11102210‡‡
<i>etr1</i>	XX0XXXXX	11010011*
	XX1XXXXX	11100022**
<i>ctr1</i>	XX0X1XXX	11011011*
	XX1X1XXX	11101022**
	XX0X0XXX	11010011†
	XX1X0XXX	11100022††
	XX0X2XXX	11012011‡
	XX1X2XXX	11102022‡‡
<i>rhd6</i>	XX0X1XXX	11011100*
	XX1X1XXX	11101101**
	XX0X0XXX	11010001†
	XX1X0XXX	11100002††
	XX0X2XXX	11012200‡
	XX1X2XXX	11102200‡‡
<i>axr2</i>	XX0X1XXX	11011100*
	XX1X1XXX	11101120**
	XX0X0XXX	11010010†
	XX1X0XXX	11100020††
	XX0X2XXX	11012200‡
	XX1X2XXX	11102210‡‡

Notes opposite

states associated with every initial state (i.e. attractors and their basins of attraction), excluding the transient states. In the model, six basins of attraction are reached. Two of them correspond to the wild-type stable activation states of atrichoblasts and trichoblasts. The other four correspond to altered patterns of root hair formation due to experimentally induced changes in ethylene availability. For comparison with the “normal” model, we also include in Table 1 the attractors of all the single loss-of-function mutants. Multiple mutants are not shown, but they can be derived from the transition tables in Fig. 3. The mutants’ phenotypes are obtained from Table 2 (see ahead).

Table 2 links the activation state of the genetic network with a root phenotype, that is itself derived from the activation states of the most downstream genes in the model (*RHD6* and *AXR2*). We have inferred the effect of these two genes on root hair development from the phenotypes of their single and double mutants, i.e. *rhd6*, *axr2* and *rhd6 axr2* plants. In Table 2 we propose a correspondence between discretized values of the *RHD6* and *AXR2* variables with the percentage of hair-bearing cells within an epidermal file. The expression levels of *RHD6* and *AXR2* are not known, but the values of Table 2 reflect the fact that these genes additively interact in determining root hair development, and that *RHD6* has a larger effect on root-hair formation than *AXR2*. For example, double mutants of these genes completely lack root hairs (Masucci & Schiefelbein, 1996; Masucci *et al.*, 1996).

← We present simulation results for wild type, and the loss-of-function mutants of all the network elements (left column). The central column contains the basins of attraction (initial states) that lead to the corresponding attractors (final steady states) in the right column. The state of the entire network is represented by a vector containing the activation states of variables *TTG*, *R homolog (Rh)*, *CPC*, *GL2*, *ETR1*, *CTR1*, *RHD6* and *AXR2*, always in this order. In the basins of attraction the initial state of the variables can be 0, 1, 2 or X (indicating any of the possible values). In the attractors, variables attain an activation state of 0, 1 or 2. Attractors marked with *, † and ‡, are those obtained in the simulations under normal ethylene, ACC and AVG treatments, respectively. Single and double symbols indicate attractors obtained in epidermal cells overlying one or two cortical cells, respectively. Thus, the genetic activation patterns of wild-type atrichoblasts and trichoblasts are marked with asterisks in the “wild-type” row.

TABLE 2

Phenotypic effect on root hair development of all the possible activation states of *RHD6* and *AXR2*, the two most downstream elements of the network model

RHD6	AXR2	% of hair-bearing cells in a file
0	0	0
0	1	10
0	2	70
1	0	20
1	1	30
1	2	90
2	0	80
2	1	90
2	2	100

Note: Not all cells in a file develop a hair; the table presents the percentage of cells in a particular file that develops a root hair depending on the activation state of *AXR2* and *RHD6*, which can be 0, 1 or 2. The table assumes that all the cells of a particular cell file have the same activation state of the corresponding regulatory network. Notice that the appearance of root hairs is a gradual response to the activity of *AXR2* and *RHD6*. Figure 4 contains a schematic representation of the root hair morphology under different genetic backgrounds.

The rightmost column of Table 2 provides the percentage of cells within a file that develop a hair for each activation state of *RHD6* and *AXR2* indicated in the first two columns of the table. Notice that (i) there is a gradual change in the appearance of root hairs depending on the values of variables *AXR2* and *RHD6*, and (ii) the precise location of the hairs within a file is not specified; thus the table describes a partially stochastic process in which cells with identical network activation states within files may or may not develop a hair. The latter is true for all cases but the extreme ones, in which none or all cells develop a hair, respectively. Figure 4 exemplifies the gradual response in root hair formation under different genetic backgrounds. Due to the scarce molecular evidence, and the large variability in the way publications report root hair number, we did not use a formal data-fitting algorithm to construct Table 2.

We report our model's predictions as the percentage of cells with hairs per file, but these predictions are sometimes hard to compare with

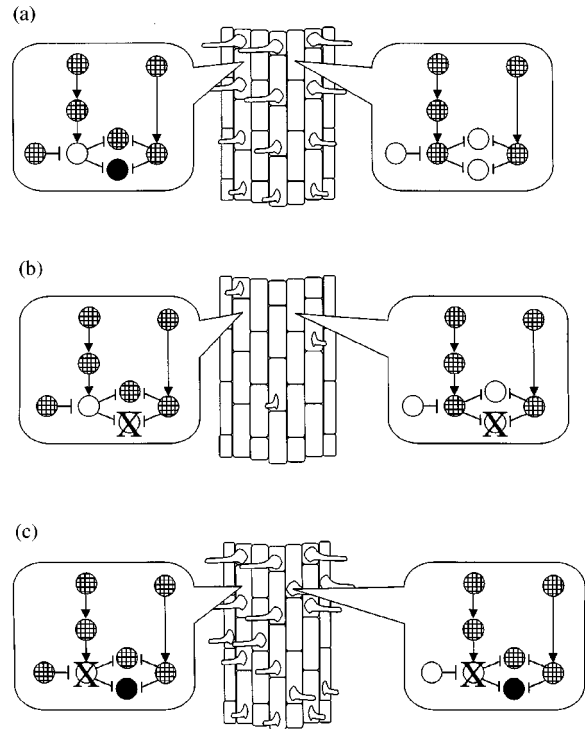


FIG. 4. Schematic representation of root hair phenotype in (a) wild-type plants, (b) *rhd6* mutants, and (c) *gl2* mutants. Steady-state activation patterns of the genetic regulatory network in epidermal cells overlying two or one cortical cells are shown on the leftmost and rightmost columns, respectively. Root epidermis cell files are illustrated in the central column. Two mutants are exemplified: one that decreases (*rhd6*) and another that increases (*gl2*) the number of epidermal root hairs without changing the total number of epidermal cells. The topology of the genetic network corresponds to that presented in Fig. 2(a). Network elements with an activation state equal to 0, 1 or 2 are represented as \circ , \oplus and \bullet , respectively. (\times) indicates which genes are mutated (loss of function).

published experimental data. The number of hairs per file varies among files within an individual root and the number of cell files per root varies among individuals. These variations should be considered when estimating the number or percentage of root hairs in the epidermis of a particular mutant. However, experimental data are not standardized to the total number of cell files per root and do not always clarify if root-hair-bearing cells are within trichoblast or atrichoblast files. Moreover, the ratio of trichoblasts to atrichoblasts in wild-type roots is not normally reported, despite that it usually varies from 0.5 to 1 (Dolan *et al.*, 1993, 1994). For

example, Table 3 shows that 42% of epidermal cells in wild-type roots have hairs. In the publication, however, the average number of files per individual is not reported. If the percentage was derived from plants with a trichoblast to atrichoblast ratio of 1, then the results would imply that 84% of the cells in a trichoblast file have a hair. The latter is the percentage that should be compared to our models' predictions. If the results were obtained from plants with a trichoblast to atrichoblast ratio of 0.72, then the same reported value of 42%, would imply that 100% of cells in the trichoblast file would have a hair. This should be kept in mind when comparing our model's predictions for percentage of root-hair-bearing cells per file with published data.

The initial state of CPC and ETR1 proteins alone determines which attractor is reached by the model. Two of the final stable states correspond to the expression patterns observed in wild-type trichoblasts and atrichoblasts. To simulate epidermal cells overlying a longitudinal anticlinal wall, CPC and ETR1 initial states are set to 1, and for the epidermal cells contacting only one cortex cell, CPC and ETR1 are set to 0 and 1, respectively. In the first type of cell, which corresponds to a trichoblast, the attractor reached is 11101121; while in the second one that corresponds to an atrichoblast, the attractor is 11011100 (Table 1). The first attractor (11101121) includes an active CPC variable, RHD6 equals 2 and AXR2 equals 1. Based on Table 2, these activation states of RHD6 and AXR2 yield a phenotype where 90% of the cells in a file develop a hair. In the second attractor (11011100), CPC, RHD6 and AXR2 are equal to 0. In this particular case, according to Table 2, none of the cells in the file with that stable activation state develop a hair. These results of the model match the phenotype of wild-type roots in which most trichoblasts develop a hair while atrichoblasts do not.

The other four attractors correspond to the simulation of pharmacological treatments on the root under a wild-type genetic background. As mentioned earlier, we may simulate ethylene or ACC treatment by setting the variable ETR1 to zero. In this case, the attractors 11100022 and 11010011 are reached in the trichoblasts and atrichoblasts, respectively. The extra availability of

ethylene in the root induces all the cells that contact anticlinal walls to develop a hair. In contrast, only 30% of the cell files that contact a periclinal wall are predicted to develop a hair. Similarly, in order to model AVG treatment we set the initial state of the variable ETR1 to 2. In this case, the attractors reached are 11102210 and 11012200 for trichoblasts and atrichoblasts, respectively. As shown in Table 2, these attractors correspond to 20 and 0% of cells in a file developing a hair, respectively. The model seems to describe accurately the change in hair to non-hair ratio due to a change in ethylene availability (Table 3).

Our regulatory network model, in contrast to previous root epidermis models (Scheres, 1996, 1997; Tanimoto *et al.*, 1995), can be used also to simulate gain- and loss-of-function mutations. In our model, mutations in all members of the ethylene receptor family ($ETR1 = 0$) cause the inactivation of CTR1 ($= 0$). In this case, the attractors reached by the model are 11100022 and 11010011, for cells overlying two and one cortical cells, respectively. According to Table 2, the phenotypes corresponding to these two attractors are 100% of hair cells if located over the anticlinal wall, and 30% of hair cells if not. The attractors of other mutations are also shown in Table 1. Simulation results for other mutants are shown in Table 3, where we compare the attractors predicted by our model for trichoblasts and atrichoblasts with published mutants and pharmacological treatments. Comparison with published results show that there is an overall good agreement among those and the simulated results. Finally, we summarize some simulation predictions for novel mutants and pharmacological treatments in Table 4.

Discussion

Cellular interactions are important during plant morphogenesis. However, the precise molecular mechanisms entailed by such interactions are only starting to be understood. Such mechanisms include how cells react to signals, and how these are integrated among cells during morphogenesis (Meyerowitz, 1997). Integrative dynamical modeling approaches will become useful to make progress in this area. In this paper, we

TABLE 3
Comparison of network simulation predictions with experimental published data

Genotype	Attractors: epidermal cells over two cortical cells (% hair cells)	Attractors: epidermal cells over one cortical cell (% hair cells)	Model predictions: predicted percentage of hair cells with respect to the WT model	Experimental evidence: average observed percentage of hair cells with respect to wild type (WT)	Model predictions: predicted percentage of ectopic hair cells with respect to WT model	Experimental evidence: average observed percentage of ectopic hair cells with respect to WT	FIT
WT	11101121 (90)	11011100 (0)	100	100 (Masucci & Schiefelbein, 1996)	0	1 (Masucci & Schiefelbein, 1996) 1.75 (Di Cristina <i>et al.</i> , 1996) 0 (Tanimoto <i>et al.</i> , 1995)	Good
WT + ACC	11100022 (100)	11010011 (30)	144.4–177.7	126 (Masucci & Schiefelbein, 1996)	23–37.5	22 (Masucci & Schiefelbein, 1996) 35–50 (Tanimoto <i>et al.</i> , 1995)	Good
WT + AVG	11102210 (20)	11012200 (0)	22.2	26 (Masucci & Schiefelbein, 1996) 0–15 (Tanimoto <i>et al.</i> , 1995)	0	0 (Masucci & Schiefelbein, 1996; Tanimoto <i>et al.</i> , 1995)	Good
<i>ttg</i>	00101121 (90)	00001121 (90)	200–300	223 (Masucci & Schiefelbein, 1996) 227 (Wada <i>et al.</i> , 1997) 200 (Hung <i>et al.</i> , 1998)	50–66.6	51 (Masucci & Schiefelbein, 1996)	Good
<i>cpc</i>	11011100 (0)	11011100 (0)	0	24 (Wada <i>et al.</i> , 1997)	0	N.A.	Fair
<i>35S::CPC</i>	11101121 (90)	11101121 (90)	200–300	312 (Wada <i>et al.</i> , 1997)	50–66.6	N.A.	Good
<i>gl2</i>	11101121 (90)	11001121 (90)	200–300	230 (Masucci & Schiefelbein, 1996) 250 (Wada <i>et al.</i> , 1997) 210 (Hung <i>et al.</i> , 1998)	50–66.6	53 (Masucci & Schiefelbein, 1996)	Good
<i>ctr1</i>	11101022 (100)	11011011 (30)	144.4–177.7	147 (Masucci & Schiefelbein, 1996)	23–37.5	32 (Masucci & Schiefelbein, 1996)	Good
<i>rhd6</i>	11101101 (10)	11011100 (0)	11.1	9 (Masucci & Schiefelbein, 1994, 1996)	0	3 (Masucci & Schiefelbein, 1994, 1996)	Fair
<i>rhd6 + ACC</i>	11100002 (70)	11010001 (10)	88.8–100	61 than WT treated with ACC (Masucci & Schiefelbein, 1994, 1996)	12.5–22.2	N.A.	Good
<i>axr2</i>	11101120 (80)	11011100 (0)	88.8	64 (Masucci & Schiefelbein, 1996)	0	0 (Masucci & Schiefelbein, 1996)	Fair
<i>axr2 + ACC</i>	11100020 (80)	11010010 (20)	111.11–133.3	64 than WT treated with ACC (Masucci & Schiefelbein, 1996)	20–33.3	N.A.	Fair
<i>ttg cpc</i>	00001121 (90)	00001121 (90)	200–300	150 (Wada <i>et al.</i> , 1997)	50–66.6	N.A.	Fair
<i>ttg gl2</i>	00101121 (90)	00001121 (90)	200–300	220 (Hung <i>et al.</i> , 1998)	50–66.6	56 (Hung <i>et al.</i> , 1998)	Good
<i>cpc gl2</i>	11001121 (90)	11001121 (90)	200–300	232 (Wada <i>et al.</i> , 1997)	50–66.6	N.A.	Good
<i>ttg rhd6</i>	00101101(10)	00001101 (10)	22.2–33.3	54 (Masucci & Schiefelbein, 1996)	50–66.6	13 (Masucci & Schiefelbein, 1996)	Fair
<i>ttg rhd6 + ACC</i>	00100002 (70)	00000002 (70)	155.5–233.3	170 (Masucci & Schiefelbein, 1996)	50–66.6	N.A.	Good
<i>ttg axr2</i>	00101120 (80)	00001120 (80)	177.7–266.6	59 (Masucci & Schiefelbein, 1996)	50–66.6	40 (Masucci & Schiefelbein, 1996)	Bad
<i>gl2 rhd6</i>	11101101 (10)	11001101 (10)	22.2–33.3	40 (Masucci & Schiefelbein, 1996)	50–66.6	4 (Masucci & Schiefelbein, 1996)	Fair
<i>gl2 rhd6 + ACC</i>	11100002 (70)	11000002 (70)	155.5–233.3	523 than <i>gl2 rhd6</i> (Masucci & Schiefelbein, 1996)	50–66.6	N.A.	Good
<i>gl2 axr2</i>	11101120 (80)	11001120 (80)	177.7–266.6	66 (Masucci & Schiefelbein, 1996)	50–66.6	25 (Masucci & Schiefelbein, 1996)	Bad
<i>ctr1 rhd6</i>	11101002 (70)	11011001 (10)	88.8–100	100 (Masucci & Schiefelbein, 1996)	12.5–22.2	Like WT (Masucci & Schiefelbein, 1996)	Good
<i>rhd6 axr2</i>	11101100 (0)	11011100 (0)	0	0 (Masucci & Schiefelbein, 1996)	0	0 (Masucci & Schiefelbein, 1996)	Good
<i>rhd6 axr2 + ACC</i>	11100000 (0)	11010000 (0)	0	0 (Masucci & Schiefelbein, 1996)	0	0 (Masucci & Schiefelbein, 1996)	Good

Note: Mutants and pharmacologically treated plants are listed in the first column. The second and third columns list the attractors predicted for epidermal cells contacting two or one cortical cells, respectively. The predicted percentage of hair-bearing cells (see Table 2) is indicated in parentheses. The fourth column includes the predicted number of hair cells with respect to wild-type model. Most values are presented within a range to take into account that the observed trichoblast to atrichoblast ratio varies from 0.5 to 1. The fifth column contains experimental evidence on the percentage of root hairs. The sixth column includes the predicted number of ectopic hairs according to our model. Again, values are presented as a range to reflect the variability of the trichoblast to atrichoblast ratio. The seventh column shows the experimental evidence on the ectopic root hairs with respect to the wild-type plants. N.A. indicates that there are no data available for the particular mutant. Finally, the eighth column includes an estimate of the agreement between the model and the experimental data. We included three qualifications, “Good” for values predicted by the model within $\pm 20\%$ of the reported data; “Fair” for values predicted by the model with $>20\%$ but in the same direction as the reported data, and finally “Bad” for predicted values that do not describe that particular mutant.

TABLE 4

Predictions of the regulatory network for mutants and pharmacological treatments not reported yet

Genotype	Attractors: epidermal cells over two cortical cells (% of hair cells)	Attractors: epidermal cells over one cortical cells (% of hair cells)	Model predictions: predicted percentage of hair cells with respect to wild-type model	Model predictions: predicted percentage of ectopic hair cells with respect to wild-type model
<i>ttg</i> + ACC	00100022 (100)	00000022 (100)	222–333	50–66.6
<i>ttg</i> + AVG	00102210 (20)	00002210 (20)	44.4–66.6	50–66.6
<i>cpc</i> + ACC	11010011 (30)	11010011 (30)	66.6–100	50–66.6
<i>cpc</i> + AVG	11012200 (0)	11012200 (0)	0	0
35S::CPC + ACC	11100022 (100)	11100022 (100)	222–333	50–66.6
35S::CPC + AVG	11102210 (20)	11102210 (20)	44.4–66.6	50–66.6
<i>gl2</i> + ACC	11100022 (100)	11000022 (100)	222–333	50–66.6
<i>gl2</i> + AVG	11102210 (20)	11002210 (20)	44.4–66.6	50–66.6
<i>ctr1</i> + ACC	11100022 (100)	11010011 (100)	222–333	50–66.6
<i>ctr1</i> + AVG	11102022 (100)	11012011 (100)	222–333	50–66.6
<i>rhd6</i> + AVG	11102200 (0)	11012200 (0)	0	0
<i>axr2</i> + AVG	11102210 (20)	11012200 (0)	22.2	0
<i>ttg cpc</i> + ACC	00000022 (100)	00000022 (100)	222–333	50–66.6
<i>ttg cpc</i> + AVG	00002210 (20)	00002210 (20)	44.4–66.6	50–66.6
<i>ttt gl2</i> + ACC	00100022 (100)	00000022 (100)	222–333	50–66.6
<i>ttg gl2</i> + AVG	00102210 (20)	00002210 (20)	44.4–66.6	50–66.6
<i>cpc gl2</i> + ACC	11000022 (100)	11000022 (100)	222–333	50–66.6
<i>cpc gl2</i> + AVG	11002210 (20)	11002210 (20)	44.4–66.6	50–66.6
<i>ttg rhd6</i> + AVG	00102200 (0)	00002200 (0)	0	0
<i>ttg axr2</i> + ACC	00100020 (80)	00000020 (80)	177.7–266.6	50–66.6
<i>tr axr2</i> + AVG	00102210 (20)	00002210 (20)	44.4–66.6	50–66.6
<i>gl2 rhd6</i> + AVG	11102200 (0)	11002200 (0)	0	0
<i>gl2 axr2</i> + ACC	11100020 (80)	11000020 (80)	177.7–266.6	50–66.6
<i>gl2 axr2</i> + AVG	11102210 (20)	11002210 (20)	44.4–66.6	50–66.6
<i>ctr1 rhd6</i> + ACC	11100002 (70)	11010001 (10)	88.8–100	12.5–22.2
<i>ctr1 rhd6</i> + AVG	11102002 (70)	11012001 (10)	88.8–100	12.5–22.2
<i>rhd6 axr2</i> + AVG	11102200 (0)	11012200 (0)	0	0
<i>cpc gl2</i> + ACC	11000022 (100)	11000022 (100)	222–333	50–66.6
<i>cpc gl2</i> + AVG	11002210 (20)	11002210 (20)	44.4–66.6	50–66.6
35S::CPC <i>rhd6</i>	11101101 (10)	11101101 (10)	22.2–33.3	50–66.6
35S::CPC <i>rhd6</i> + ACC	11100002 (70)	11100002 (70)	155.5–233.3	50–66
35S::CPC <i>rhd6</i> + AVG	11102200 (0)	11102200 (0)	0	0

Note: The table contains the same kind of information as the first, second, third, fourth, and sixth columns in Table 3.

have proposed a model for a mechanism by which cells transduce extra-cellular signals, via the genetic regulatory network that controls cell fate determination in the root epidermis.

We presented a simple discrete-state model. However, theoretical studies show that the number and type of stable states found in discrete systems are the same as those attained with appropriate equivalent continuous models (Bagley & Glass, 1996; Glass, 1975; Glass & Kauffman, 1973). It is noteworthy, that in contrast to our previous *Arabidopsis* network models, this one does not include any feedback loops. The

presence of functional positive feedback loops is a pre-requisite to obtain multistationarity, which is necessary to attain different stable states that represent the genetic activation patterns observed in different cell types (Thieffry *et al.*, 1995; Thomas, 1991). In the network model presented here, cellular differentiation depends upon the initial activation states of two elements of the model, the proteins CPC and ETR1, which are assumed to depend on a signaling mechanism external to the network. This mechanism does not preclude the possibility that future studies uncover new genes and interactions including

some positive functional loops, which may reinforce the cell patterning process simulated by the model that we present here.

Our model makes two basic assumptions concerning the signals involved in cell fate determination in the root epidermis. Both are based on experimental data that show that the contact of epidermal cells with a longitudinal anticlinal cortex wall is critical for root hair development (Scheres, 1996, 1997), and that the initial state of the CPC protein depends on the position of the epidermal cell relative to cortex cells. A similar mechanism has been proposed before by Scheres (1997). This assumption implies that an unknown signal activates or makes the CPC protein available in those cells that will become trichoblasts. A cell wall component, for example a glycoprotein, rather than a diffusible molecule could be involved in such a mechanism. A key pre-requisite for that component is its localization along the longitudinal anticlinal walls of cortex cells. This type of expression pattern has been documented already in cells of *Arabidopsis* roots for some carbohydrates (Freshour *et al.*, 1996).

Second, we assume in our model that ethylene is a signaling molecule uniformly available to all epidermal cells. Thus, ethylene does not convey by itself positional information during sub-specification of epidermal cell-types. In contrast, some previous models assume that ethylene (or ACC) diffuses only through longitudinal anticlinal walls of cortical cells, inducing root hair development only in epidermal cells that are in direct contact with the cleft (Scheres, 1997; Tanimoto, 1995). The fact that in the absence of *TTG* and *GL2*, hair formation in AVG-treated roots occurs in the right place, partially supports the pre-patterning role of ethylene. However, there are two experimental results that challenge such a hypothesis. The first one comes from a trichoblast that divides longitudinally to yield two daughter cells, from which one becomes an atrichoblast (Berger *et al.*, 1998b). If a diffusible signal determined the trichoblast fate, then both daughter cells should attain this fate. One could still argue for a diffusible signal that could only maintain the trichoblast fate in one cell and not the other, but this mechanism does not seem a plausible one. The second piece of evidence is that an atrichoblast remains as such even if

surrounding trichoblasts, atrichoblasts or cortical cells are ablated (Berger *et al.*, 1998a). With such experimental manipulation, any gradient of a diffusible morphogen should have been destroyed thus increasing ethylene availability. This in turn would have caused that isolated atrichoblast to differentiate into a trichoblast.

Previous authors have proposed static schematic representations of the gene interactions involved in cell-type determination in the *Arabidopsis* root epidermis (Scheres & Wolkenfelt, 1998; Schiefelbein, 1998; Schiefelbein *et al.*, 1997). These authors have proposed the same architecture of interactions among the genes encoding *TTG*, *GL2*, and R homolog that we present here. Also, it was previously proposed that CPC is upstream of *GL2* (Wada *et al.*, 1997). However, we propose that the ethylene response pathway is independent of the *GL2* pathway, although both converge in the negative regulation of downstream elements such as *AXR2* and *RHD6* [see Fig. 2(a)]. In contrast, most previous authors have postulated that the ethylene response pathway is downstream and repressed by *GL2* (see, for example, Schiefelbein *et al.*, 1997). However, loss-of-function mutations, either on the ethylene receptor family or on *CTR1* (Hua & Meyerowitz, 1998; Kieber *et al.*, 1993) develop root hairs in all epidermal cells, evidencing that the ethylene response pathway is active even in cells expressing *GL2*. Therefore, *GL2* cannot be a repressor of the ethylene pathway [see Fig. 2(a)].

Our architecture is also compatible with phenotypes of *ttg* and *gl2* mutants treated with the ethylene synthesis inhibitor, AVG (Masucci & Schiefelbein, 1996). It is noteworthy that in some previous papers these experiments have been used to postulate that the ethylene response pathway is downstream of *GL2* (Scheres, 1997; Schiefelbein *et al.*, 1997). Finally, loss-of-function mutants of the ethylene receptor family, namely the *etr1 etr2 ein4 ers2* quadruple mutants, have a constitutive ethylene response phenotype, like that of *ctr1* mutants (Hua & Meyerowitz, 1998). This phenotype is also compatible with the model presented here, but not with previous ones (see Tanimoto *et al.*, 1995).

In brief, our model is a new proposition of the regulatory interactions between genes and proteins controlling root hair development. Notably,

it establishes that the transduction pathway of ethylene is parallel, and not downstream, of the group of transcription factors that control root hair appearance. Finally, it is a dynamic model that can be used to describe and predict the stable expression patterns, under wild type, mutants and pharmacologically treated roots, of a group of proteins and molecules controlling root hair development.

The overall agreement of published and simulated results (Table 3) suggests that this first dynamical model captures key elements involved in the genetic regulation of cell fate determination in the epidermis. It is important to consider that the experimental results have a large standard deviation that we did not include in the table (see for example, Masucci and Schiefelbein, 1996; Masucci *et al.*, 1996). In all but two cases, however, the phenotypes predicted by the model are very close to the average observed phenotypes. The two cases in which the predicted and observed phenotypes are quite different: *ttg axr2* and *gl2 axr2* double mutants. The total number of observed hair cells is not accurately described by our model, although the percentage of ectopic hairs is close to the experimental evidence. A partial solution for the discrepancies would be solved by including a non-zero activity for *GL2* in the absence of the normal activation coming from *TTG*. In fact, there is some experimental evidence that supports such activity (Huang *et al.*, 1998), but we did not include it because we could not identify the putative upstream regulatory gene responsible for such *GL2* activity. Certainly, a *TTG*-independent *GL2* activation pathway would reduce *RHD6* activity and hence the number of hairs predicted for a *ttg axr2* mutant would be lower and would be more similar to the phenotype observed for this double mutant. In any case, this discrepancy between our model and the experimental data suggests that there must be such an alternative pathway that should be sought experimentally. On the other hand, including in the model an additional inhibitory pathway over *RHD6*, independent of *TTG* and *GL2*, might yield a more accurate prediction of the phenotype of the *gl2 axr2* mutant. There is no evidence for such a pathway, but this should be looked for in future experimental work.

We still need much more molecular and genetic data to further elaborate the model. For example, it is known that the gene *ROOT HAIR-LESS 1 (RHL1)* is an important gene involved in root hair formation (Schneider *et al.*, 1998). Nevertheless, we were unable to include this and other genes in the analysis because the appropriate multiple mutations and molecular evidence are still not available. Furthermore, available data already suggest that there are missing genes in the network proposed here. For example, the phenotype of *cpc ttg* double mutants suggests that *GL2* has a basal expression level in the absence of the inhibition of the CPC active protein and the activation of *TTG/R*-homolog pathway. This suggests that there is another activator of *GL2* yet to be discovered.

There is another relevant issue regarding the interpretation of our model. The network includes many of the regulatory genes that control the appearance of root hairs, but does not incorporate the most downstream target genes and biochemical pathways that directly affect the morphological cellular processes underlying hair formation. Thus, a stable activation pattern of the network represents the activity only of some key regulatory genes. These regulatory genes trigger the activation and inhibition of many non-modeled downstream pathways, which in turn determine the cellular fate of the epidermal cell. For example, the activity of the CPC network element results in the inhibition of *GL2*, causing the de-repression of *AXR2* and *RHD6*, which form part of the proteins leading to the appearance of root hair. In other words, the molecular events determine the cellular fate. In contrast, some authors imply in their schematic representations that the cellular fate determines the activation state of some of the genes that are themselves responsible for cell fate determination (see, for example, Fig. 1 of Schiefelbein, 1998), such circular schematic models may lead to considerable confusion.

Network models like the one presented here are not appropriate for analysing transient states of cell differentiation during development. Cell differentiation in the root epidermis is a continuous process. Macroscopic differences between trichoblasts and atrichoblasts appear early during development (Dolan *et al.*, 1993, 1994).

At the proximal end of the root apical meristem epidermal cells stop dividing and start rapid elongation. Finally, epidermal cells cease to grow and trichoblasts and develop root hairs, thus defining the differentiation root zone. At this stage, epidermal cells reach a stable state and are considered to be mature. Different genes seem to control different stages of this process. For example, while *TTG* seems to act early, ethylene seems to act late (see Scheres, 1996, 1997). However, once cells reach the stable mature state of differentiation, the activity of such genetic products should also reach a stable steady state. Discrete network models are suitable for the prediction of such stable genetic regulatory patterns observed in mature cells. In the model presented here, the steady states correspond to the genetic profiles of trichoblasts and atrichoblasts in the root epidermis. Therefore, the morphological interpretation of our genetic regulatory network corresponds only to the differentiation region of the root. Consequently, our model may not simulate the transitory stages of development and does not consider explicitly the gradient of cellular differentiation that exists from the root meristem towards the hypocotyl.

The rapid progress in genetic and experimental approaches will eventually provide the data to detail the molecular pathways and cellular mechanisms that determine cell fate, cell shape and cell division during organ development. Also, they will help to understand how these pathways are integrated and modulated by external signals. However, formal approaches will become necessary to provide rigorous spatio-temporal frameworks to integrate data, and also to elaborate predictions that link the genetic circuitry underlying development with the final morphology of an organism. Network models will become useful to link regulatory interaction with other models that explicitly consider the spatial and cellular scales. For example, Mjolsness *et al.* (1991) proposed a model that couples a neural network to a grammatical model of cellular differentiation. However, these authors did not apply their model to any particular biological system. In this paper, we have shown that cell fate in the root epidermis is largely determined by positional signaling. Future models should explicitly incorporate such a spatial component using cellular

automata (Ermentrout & Edelstein-Keshet, 1993) or L-systems (Prusinkiewicz & Lindenmayer, 1990).

Thanks to Ben Scheres, Caroline Burgett, Joseph Dubrovsky and Francisca Acevedo for their comments in the preparation of this manuscript. This work was supported by a UNAM scholarship to L.M., and a grant from the Mexican Council of Science and Technology (CONACYT 3667 P-N) to E.R.A.B.

REFERENCES

- BAGLEY, R. J. & GLASS, L. (1996). Counting and classifying attractors in high dimensional dynamical systems. *J. theor. Biol.* **183**, 269–284.
- BERGER, F., HASELOFF, J., SCHIEFELBEIN, J. & DOLAN, L. (1998a). Positional information in root epidermis is defined during embryogenesis and acts in domains with strict boundaries. *Curr. Biol.* **8**, 421–430.
- BERGER, F., HUNG, C. Y., DOLAN, L. & SCHIEFELBEIN, J. (1998b). Control of cell division in the root epidermis of *Arabidopsis thaliana*. *Dev. Biol.* **194**, 235–245.
- BODNAR, J. W. (1997). Programming the *Drosophila* embryo. *J. theor. Biol.* **188**, 391–445.
- CLARK, K. L., LARSEN, P. B., WANG, X. & CHANG, C. (1998). Association of the *Arabidopsis* CTR1 Raf-like kinase with the ETR1 and ERS ethylene receptors. *Proc. Nat. Acad. Sci. U.S.A.* **95**, 5401–5406.
- COEN, E. S. & MEYEROWITZ, E. M. (1991). The war of the whorls: genetic interactions controlling flower development. *Nature* **353**, 31–37.
- DI CHRISTINA, M., SESSA, G., DOLAN, L., LINSTEAD, P., BAIMA, S., ROBERTI, I. & MORELLI, G. (1996). The *Arabidopsis* Athb-10 (GLABRA2) is an HD-Zip protein required for regulation of root hair development. *Plant J.* **10**, 393–402.
- DOLAN, L., JANMAAT, K., WILLEMSSEN, V., LINSTEAD, P., POETHIG, S., ROBERTS, K. & SCHERES, B. (1993). Cellular organization of the *Arabidopsis thaliana* root. *Development* **119**, 71–84.
- DOLAN, L., DUCKETT, C. M., GRIERSON, C., LINSTEAD, P., SCHNEIDER, K., LAWSON, E., DEAN, C., POETHIG, S. & ROBERTS, K. (1994). Clonal relationships and cell patterning in the root epidermis of *Arabidopsis*. *Development* **120**, 2465–2474.
- ERMENTROUT, G. B. & EDELSTEIN-KESHET, L. (1993). Cellular automata approaches to biological modeling. *J. theor. Biol.* **160**, 97–133.
- FLUHR, R. (1998). Ethylene perception: from two-component signal transducers to gene induction. *Trends Plant Sci.* **3**, 141–146.
- FRESHOUR, G., CLAY, R. P., FULLER, M. S., ALBERSHEIM, P., DARVILL, A. G. & HAHN, M. G. (1996). Developmental and tissue-specific structural alterations of the cell-wall polysaccharides of *Arabidopsis thaliana* roots. *Plant Physiol.* **110**, 1413–1429.
- GALWAY, M. E., MASUCCI, J. D., LLOYD, A. M., WALBOT, V., DAVIS, R. W. & SCHIEFELBEIN, J. W. (1994). The *TTG* gene is required to specify epidermal cell fate and cell patterning in the *Arabidopsis* root. *Dev. Biol.* **166**, 740–754.

- GLASS, L. (1975). Classification of biological networks by their qualitative dynamics. *J. theor. Biol.* **54**, 85–107.
- GLASS, L. & KAUFFMAN, S. A. (1973). The logical analysis of continuous, non-linear biochemical control networks. *J. theor. Biol.* **39**, 103–129.
- HUA, J., CHANG, C., SUN, O. & MEYEROWITZ, E. M. (1995). Ethylene insensitivity conferred by *Arabidopsis* ERS gene. *Science* **269**, 1712–1714.
- HUA, J. & MEYEROWITZ, E. M. (1998). Ethylene responses are negatively regulated by a receptor gene family in *Arabidopsis thaliana*. *Cell* **94**, 261–271.
- HUNG, C. Y., LIN, Y., ZHANG, M., POLLOCK, S., MARKS, M. D. & SCHIEFELBEIN, J. (1998). A common position-dependent mechanism controls cell-type patterning and *GLABRA2* regulation in the root and hypocotyl epidermis of *Arabidopsis*. *Plant Physiol.* **117**, 73–84.
- KAUFFMAN, S. A. (1993). *The Origins of Order: Self-Organization and Selection in Evolution*. Oxford: Oxford University Press.
- KIEBER, J. J. (1997). The ethylene response pathway in *Arabidopsis*. *Annu. Rev. Plant Physiol. Plant Mol. Biol.* **48**, 227–296.
- KIEBER, J. J., ROTHENBERG, M., ROMAN, G., FELDMANN, K. A. & ECKER, J. R. (1993). *CTR1*, a negative regulator of the ethylene response pathway in *Arabidopsis*, encodes a member of the Raf family of protein kinases. *Cell* **72**, 427–441.
- MASUCCI, J. D., RERIE, W. G., FOREMAN, D. R., ZHANG, M., GALWAY, M. E., MARKS, M. D. & SCHIEFELBEIN, J. W. (1996). The homeobox *GLABRA2* is required for position-dependent cell differentiation in the root epidermis of *Arabidopsis thaliana*. *Development* **122**, 1253–1260.
- MASUCCI, J. D. & SCHIEFELBEIN, J. W. (1996). Hormones act downstream of *TTG* and *GL2* to promote root hair outgrowth during epidermis development in the *Arabidopsis* root. *Plant Cell* **8**, 1505–1517.
- MENDOZA, L. & ALVAREZ-BUYLLA, E. R. (1998). Dynamics of the genetic regulatory network for *Arabidopsis thaliana* flower morphogenesis. *J. theor. Biol.* **193**, 307–319.
- MENDOZA, L., THIEFFRY, D. & ALVAREZ-BUYLLA, E. R. (1999). Genetic control of flower morphogenesis in *Arabidopsis thaliana*: a logical analysis. *Bioinformatics* **15**, 593–606.
- MJOLSNES, E., SHARP, D. H. & REINITZ, J. (1991). A connectionist model of development. *J. theor. Biol.* **152**, 429–453.
- MEYEROWITZ, E. M. (1994). The genetics of flower development. *Sci. Am.* **271**, 40–47.
- MEYEROWITZ, E. M. (1997). Plants and the logic of development. *Genetics* **145**, 5–9.
- PIGLIUCCI, M. (1996). How organisms respond to environmental changes: from phenotypes to molecules (and vice versa). *Trends Ecol. Evol.* **11**, 168–173.
- PRUSINKIEWICZ, P. & LINDERMAYER, A. (1990). *The Algorithmic Beauty of Plants*. New York: Springer-Verlag.
- REINITZ, J. & SHARP, D. H. (1995). Mechanism of formation of eve stripes. *Mech. Dev.* **49**, 133–158.
- SCHERES, B. (1996). Embryo patterning genes and reinforcement cues determine cell fate in the *Arabidopsis thaliana* root. *Seminars Cell & Dev. Biol.* **7**, 857–865.
- SCHERES, B. (1997). Cell signaling in root development. *Curr. Op. Genet. & Dev.* **7**, 501–506.
- SCHERES, B. & WOLKENFELT, H. (1998). The *Arabidopsis* root as a model to study plant development. *Plant Physiol. Biochem.* **36**, 21–32.
- SCHIEFELBEIN, J. (1998). Cell-fate specification in the root epidermis. *Trends Plant Sci.* **3**, 3–4.
- SCHIEFELBEIN, J. W., MASUCCI, J. D. & WANG, H. (1997). Building a root: the control of patterning and morphogenesis during root development. *Plant Cell* **9**, 1089–1098.
- SCHNEIDER, K., MATHUR, J., BOUDONCK, K., WELLS, B., DOLAN, L. & ROBERTS, K. (1998). The *ROOT HAIRLESS 1* gene encodes a nuclear protein required for root hair initiation in *Arabidopsis*. *Genes Dev.* **12**, 2013–2021.
- TANIMOTO, M., ROBERTS, K. & DOLAN, L. (1995). Ethylene is a positive regulator of root hair development in *Arabidopsis thaliana*. *Plant J.* **8**, 943–948.
- THIEFFRY, D., SNOUSSI, E. H., RICHELLE, J. & THOMAS, R. (1995). Positive loops and differentiation. *J. Biol. Syst.* **3**, 457–466.
- THOMAS, R. (1991). Regulatory networks seen as asynchronous automata: a logical description. *J. theor. Biol.* **153**, 1–23.
- VAN DEN BERG, C., WEISBEEK, P. & SCHERES, B. (1998). Cell fate and cell differentiation status in the *Arabidopsis* root. *Planta* **205**, 483–491.
- WADA, T., TACHIBANA, T., SHIMURA, Y. & OKADA, K. (1997). Epidermal cell differentiation in *Arabidopsis* determined by a Myb homolog, *CPC*. *Science* **277**, 1113–1116.
- WADA, T., TACHIBANA, T., SHIMURA, Y. & OKADA, K. (1998). Expression pattern of *CPC* and its role in the differentiation of root hairs. In: *Proceedings of the 9th International Conference on Arabidopsis Research*, p. 487.
- WEIGEL, D. & MEYEROWITZ, E. M. (1993). Activation of floral homeotic genes in *Arabidopsis*. *Science* **261**, 1723–1726.